Evidence of humic acid-aluminium-silicon complexes under controlled conditions

Patricia Merdy, Jean-Dominique Meunier, Fabio Ziarelli, Yves Lucas

▶ **To cite this version:**

Patricia Merdy, Jean-Dominique Meunier, Fabio Ziarelli, Yves Lucas. Evidence of humic acid-aluminium-silicon complexes under controlled conditions. Science of the Total Environment, 2022, 829, pp.154601. 10.1016/j.scitotenv.2022.154601 . hal-03967824

HAL Id: hal-03967824
https://hal.science/hal-03967824v1

Submitted on 1 Feb 2023

HAL is a multi-disciplinary open access archive for the deposit and dissemination of scientific research documents, whether they are published or not. The documents may come from teaching and research institutions in France or abroad, or from public or private research centers.

L'archive ouverte pluridisciplinaire **HAL**, est destinée au dépôt et à la diffusion de documents scientifiques de niveau recherche, publiés ou non, émanant des établissements d'enseignement et de recherche français ou étrangers, des laboratoires publics ou privés.

Distributed under a Creative Commons Attribution - NonCommercial - NoDerivatives 4.0 International License

Evidence of humic acid-aluminium-silicon complexes under controlled conditions

Patricia Merdy[a*], Jean-Dominique Meunier[b], Fabio Ziarelli[c], Yves Lucas[a]

[a] Université de Toulon, Aix Marseille Univ, CNRS, IM2NP, 83041 Toulon CEDEX 9, France
[b] CEREGE, CNRS, Aix-Marseille Univ, IRD, INRAE, 13545 Aix-en-Provence, France
[c] Aix Marseille Univ, CNRS, Centrale Marseille, FSCM, FR1739, 13013, Marseille, France

*Corresponding author (merdy@univ-tln.fr)

HIGHLIGHTS

- First evidence of OM-metal-Si complex impacting environmental dynamics
- Si alone actually interacts with humic acid (HA), but weakly
- With both Si and Al, HA-Al-Si complex with bridging Al and Al-O-Si bond
- Si promotes the maintenance of both Al and HA in solution
- Such complexes likely exist with other metals (Fe, Mn) and metalloids (As, Ge)

GRAPHICAL ABSTRACT

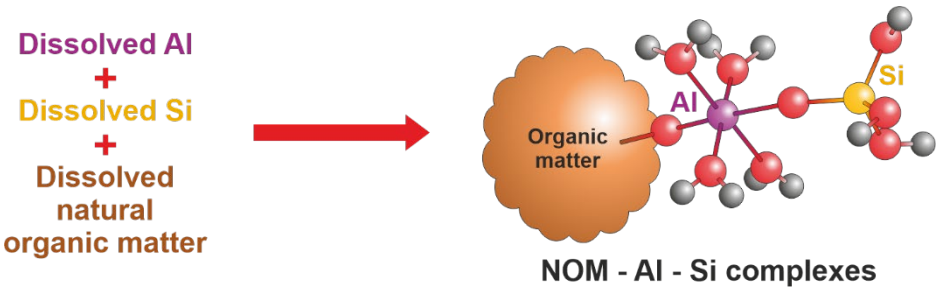

ABSTRACT

The chemistry of silicon (Si), the second most abundant element in soil after oxygen, is not yet fully understood in the soil-water-plant continuum. Although Si is widely accepted as an element that has little or no interaction with natural organic matter, some data seems to show the opposite. To identify a potential interaction between natural organic matter and Si, batch experiments were achieved at various pH and Si concentrations, involving also Al^{3+} as a common ion in soil and using humic acid (HA) as a typical model for natural organic matter. Several complementary techniques were used to characterize the possible complexes formed in the dissolved or solid phases: molecular fluorescence spectroscopy, ^{29}Si solid-state NMR, Fourier transform infrared spectroscopy, quantification of Si, Al and organic carbon, and nanoparticle size distribution. These tools revealed that humic acid indeed interacts, but weakly, with Si alone. In the presence of Al, however, a ternary complex HA-Al-Si forms, likely with Al as the bridging atom. The presence of Si promotes the maintenance of both Al and DOM in solution, which is likely to modify the result or the kinetics of pedogenesis. Such complexes can also play a role in the control of Al toxicity towards plants and probably also exists with other metals, such as Fe or Mn, and other metalloids such as As.

Keywords

Silicon, Humic acid, Complexation, Spectroscopy, Nanocolloids, Sorption sites

1. Introduction

Silicon-carbon interaction is a subject of interest in many disciplines. The synthesis of organosilicon compounds has given rise to products of daily use such as silicone or silsesquioxanes with many applications in industrial chemistry, agriculture and medicine (Larina, 2021). It has long been known that life is able to manipulate silicon for various purposes, for example forming sponge spicules, diatom frustules or plant phytoliths (Perry, 2015). Plants have several types of membrane transport proteins (Ma and Yamaji, 2015), and the polymerization of silica is carried out thanks to enzymes such as silicatein in sponges (Cha et al., 1999; Shimizu and Morse, 2018) or to small peptides such as silaffins in diatoms (Otzen, 2012). Recently, it has been shown that carbon-silicon bonds can be formed by biocatalysis carried out by bacteria modified by direct evolution, which increases the capacities of living systems (Kan et al., 2016). However, these latter authors pointed out that carbon-silicon bond formation is unknown in nature.

In the terrestrial ecosystem, the biogeochemical cycle of Si is largely documented and presents mostly inorganic chemical reactions (Schaller et al., 2021). The weathering of primary or secondary silicate minerals is the primary source of dissolved Si. Among secondary silicate minerals, phytoliths from plant Si recycling (Lucas et al., 1993) play a key role due to their high solubility (Cornelis et al., 2011; Keller et al., 2012). Soluble Si in soils is mostly in the form of bioavailable orthosilicic acid (H_4SiO_4). It is indeed this species which is absorbed by the roots (Jones and Handreck, 1967) and which is found in the xylemic sap of plants (Mitani et al., 2005). It precipitates in the plant tissue in biogenic opal, forming phytoliths. If the soil solution is oversaturated with Si, for example due to evaporation or freezing, the orthosilicic acid rapidly precipitates in the form of clay minerals or, where dissolved Al is not available, in the form of hydrated opal or siliceous gel (Sommer et al., 2006), with possible transitional formation of polymerized silicic acid species (Wonish et al., 2008). The existence of natural organosilicon compounds in the soil-water-plant continuum is a subject of controversy. Some studies suggested the existence of such compounds (Kolesnikov and Gins, 2001; Inanaga et al., 1995; Matychenkov et al., 2016; Bennett et al., 1991; Bennett, 1991) while others did not find evidence of them (Peggs and Bowen, 1984; Exley, 1998; Viers et al., 1997; Viers et al., 2000). Recent studies motivated by the growing concern for the treatment of polluted sites or effluents have empirically shown the impact of the Si-organic matter association on the dynamics of metals or metalloids, without mechanistic processes having been identified (Li and al., 2019; Ma et al., 2021; Zhao et al., 2022).

In the present study, we are questioning the nature of interactions between natural organic matter and Si in the form of orthosilicic acid. In particular, we wonder if the complexation of Si by ligands of natural organic matter would increase the overall Si solubility in the soil solution. While interactions between dissolved organic molecules and Si have been shown to exist, leading to accelerated dissolution of quartz, it is mainly adsorption processes that have been mentioned (Bennet, 1991). Studies on complexation between Si and natural organic matter in solution are very few and seem to show, or to hypothesize, the absence of complexation between Si and organic molecules, or the presence of weak complexes when they exist. For example, the study by Poulson (1997) could not prove the existence of an oxalate-Si complex after titration of $Si(OH)_4$ by $K_2C_2O_4$. Potentiometric titration experiments were performed by Ohman et al. (1991) in homogeneous solutions of Si(OH)4 and catechol, showing the existence

above pH 7 of a hexacoordinated complex, SiL_3^{2-}, where L is the catechol ligand. Inanaga and Okasaka (1995) have shown that silicon can combine with lignin-carbohydrate complexes in cell walls of rice shoots, but the corresponding species has not been identified. Pokrovski and Schott (1998) reported that Si formed weak complexes in solution with simple organic ligands having carboxylic or phenolic functional groups. Kambalina et al. (2014), however, concluded after spectrophotometric measurements that Si does not form stable complexes with fulvic and humic acids in weak-acid media (pH 3-4).

In the present study, we used several complementary techniques to identify possible species in which Si is bound to natural organic matter. Batch tests were performed using humic acid (HA), taken as a model of natural soil organic matter, and dissolved Si, under different conditions of concentration and pH. We have considered the presence of Al^{3+} species in the systems, as aluminium is a very common element present in soil and highly reactive with Si. The products formed in the batch tests were analyzed by molecular fluorescence, IRTF and ^{29}Si solid-state NMR spectroscopies, along with Si, Al and organic carbon quantifications.

2. Material and methods

2.1. Batch systems

An HA solution at 120 mg L^{-1} was prepared from a commercial powder (Humic Acid, Alfa Aesar, 41747). Si and Al stock solutions were prepared from Na2SiO3 (Carlo Erba Reagenti, 373908) and $Al(NO_3)_3.9H_20$ (Merck, 1.01063.0500), respectively. Three systems were studied: HA-Si, HA-Al and HA-Si-Al. For each system, 15 solutions (S01 to S15) were prepared with an HA concentration equal to 120 mg L^{-1} and Si or Al concentrations varying from 0 to 10^{-2} mol L^{-1} according to concentrations given in Table 1. This concentration range includes the concentrations range observed in most natural surface waters (soil solutions, rivers and lakes) for dissolved Si (Cornelis et al., 2011) and Al (Lindsay and Walthall, 2020). After component mixing, each solution was left to equilibrate for one week. Precipitation occurred in some of the solutions, these are indicated in the results section. All experiments with the associated measurements were repeated three times to ensure reliability.

Table 1
Si or Al concentrations in the HA-Si, HA-Al or HA-Si-Al systems. In the HA-Si-Al system, both Si and Al are at the given concentration.

Suffix of the solution	S01	S02	S03	S04	S05	S06	S07	S08	S09	S10	S11	S12	S13	S14	S15
Concentration mol L^{-1}	$1\ 10^{-2}$	$8\ 10^{-3}$	$6\ 10^{-3}$	$3\ 10^{-3}$	$1\ 10^{-3}$	$8\ 10^{-4}$	$6\ 10^{-4}$	$3\ 10^{-4}$	$1\ 10^{-4}$	$8\ 10^{-5}$	$6\ 10^{-5}$	$3\ 10^{-5}$	$1\ 10^{-5}$	$1\ 10^{-6}$	0

2.2. Fluorescence spectroscopy

Fluorescence spectroscopy is an interesting tool for studying complex molecules such as natural organic matter since it emits natural fluorescence under excitation and the fluorescence is sensitive to the physicochemical properties of the solution.

2.2.1. Fluorescence excitation-emission matrix (EEM)

In EEM measurements the emission signal is registered on a wavelength range, at every step of the range of an excitation wavelength, resulting in a three-dimensional contour plot of fluorescence intensity as a function of excitation and emission wavelengths, commonly called an excitation-emission matrix (EEM). The maximum intensity peaks observed on an EEM can be related to fluorophores defined by a pair of emission and excitation wavelengths (λ_{ex}, λ_{em}). The emission-excitation coordinates of the peaks can reveal the origin of the organic matter (terrestrial, marine, fresh water), as described by Coble (1996).

EEMs were obtained from two series of 12 samples for each system (HA-Si, HA-Al and HA-Si-Al), whose Si and Al concentrations varied from 10^{-2} to 10^{-6} M, which were adjusted to pH 4, 7 and 9 using HCl solutions (0.1 M, HCl Trace Metal Grade 37% v/v from Fisher Scientific) and/or NaOH (0.1M, Crystals from Sigma-Aldrich). The solutions were diluted by a factor of 10 before fluorescence measurement. Preliminary experiments were carried out to avoid inner screen effect, using a sample dilution followed by checking the proportional signal intensity response (data not shown).

The measurement was performed using a Hitachi model F-4500 spectrophotometer, equipped with a 450 W xenon lamp. Sample solutions were placed in 1 cm x 1 cm quartz cells. The excitation window was set at 5 nm and the emission window at 10 nm. The excitation wavelengths ranged from 200 nm to 500 nm, and emission wavelengths from 250 nm to 600 nm, with a 5 nm step at a scan rate of 2400 nm min^{-1} for both. The photomultiplier was set to 700 V.

2.2.2. Fluorescence quenching or enhancement

This technique consists of following the change of the fluorescence intensity of a fluorophore during the gradual addition of Si, Al or both together. For natural organic matter such as HA, this change indicates the formation of a complex between the fluorophore and the added compound (static quenching or enhancement) (Luster et al., 1996). It allows calculation of the complexing capacities and the apparent stability constants of the fluorescence ligand (Ryan and Weber, 1982).

We recorded the fluorescence intensity of the HA fluorophore that had the higher intensity without an added compound as a function of Si, Al or both together at three pH (4, 7 and 9) adjusted with HCl and NaOH, which were preferred over the usual buffers in order to avoid any impact on the fluorescence signal (Merdy et al., 2020). During the fluorescence quenching experiment, it checks should be made for the absence of solid precipitation after each addition of Si or Al. This was done after equilibrating the solutions for at least three hours by visual inspection of the solutions and by measuring the amount of residual carbon in batch sample after filtration.

2.3. Organic carbon analysis

The batch samples were filtered through glass fiber filters (0.7 µm, GF/F Whatman) previously treated at 450°C to get rid of any traces of organic carbon. In the resulting filtrate, the dissolved organic carbon (DOC) concentration was measured using a TOC-VCSH analyzer (Shimadzu) coupled to an ASI-V auto-sampler (Shimadzu). The particulate organic carbon (POC) remaining on the filters

was quantified using a Thermo Flash 2000 Elemental Analyzer in NC mode (ThermoScientific).

2.4. Infrared spectroscopy

The precipitates obtained after filtration of batch samples were analyzed by IR spectroscopy in order to identify vibration frequencies that could clarify the nature of the bonds between Si and HA in the solid phases . Infrared spectra were recorded using a JASCO FT/IR-410 spectrometer over a range from 400 to 4000 cm^{-1} in steps of 1 cm^{-1}. The pellets used in the analysis were obtained using a hydraulic press exerting a pressure of 5000 psi for approximately one minute. They were prepared from KBr (powder, Sigma-Aldrich). Only samples presenting enough solids on the filter could be analyzed in solid-state infrared.

2.5. Si and Al quantification

Dissolved Si was quantified using a DR2800 (Hach Lange) spectrophotometer. An assay kit (Method 8186, Hach Lange) was used to apply a colorimetric method based on the formation of the blue Cr-Si complex, a method adapted from "Standard Methods for the Examination of Water and Wastewater" (Greenberg, 1992). Dissolved Al was quantified with a Shimadzu UV-1800 spectrophotometer using the chromazurol S reagent (2.10^{-4} mol L^{-1}, powder, VWR) in hexamine buffer (0.2 mol L^{-1}, powder, VWR) at pH 4.9, adjusted with HCl (37% v/v Trace Metal Grade, Fisher Scientific) (Kennedy and Powell, 1986).

2.6. Colloid size distribution

The colloid size distribution was determined by Nano Tracking Analysis (NTA) using a Malvern NS500 apparatus. This technique tracks individual colloidal particles in the liquid and relates the rate of Brownian motion to the particle size. The tracking of a sufficient number of particles allows particle size distribution and concentration to be obtained. The NTA analysis was performed on samples whose concentrations were 120 mg L^{-1} for HA, 10^{-3} M for Si and 10^{-3} M for Al.

2.7. Solid-state NMR of ^{29}Si

The solid-state NMR of ^{29}Si was used to supplement the data obtained by IR spectroscopy. NMR spectra were determined on powders obtained after centrifugation of a sufficiently large volume of batch solutions prepared at pH 7 using 120 mg L^{-1} of HA and 10^{-2} mol L^{-1} Si or Al concentrations.

All solid-state NMR spectra were obtained on a Bruker Avance-400 MHz NMR spectrometer operating at ^{29}Si resonance frequency of 79.5 MHz. About 20 mg of samples were placed in zirconium dioxide rotors with a 4-mm outer diameter and spun at a Magic Angle Spinning rate of 10 kHz in a commercial Bruker Double Channel probe. ^{29}Si CPMAS experiments were performed with the Cross Polarization (CP) technique (Schaefer and Stejskal, 1976) using a ramped 1H-pulse starting at 100% power and decreasing to 50% during the contact time (5 ms) in order to circumvent Hartmann-Hahn mismatches (Peersen et al., 1993; Cook et al., 1996). To improve the resolution, a dipolar decoupling GT8 pulse sequence (Gerbaud et al., 2003) was applied during the acquisition time.

To obtain a good signal-to-noise ratio, between 10^3 and 10^4 scans were accumulated using a delay of 2.5 s. The ^{29}Si chemical shifts were referenced to tetramethylsilane.

3. Results and discussion

3.1. Fluorescence spectroscopy and precipitations in the different systems

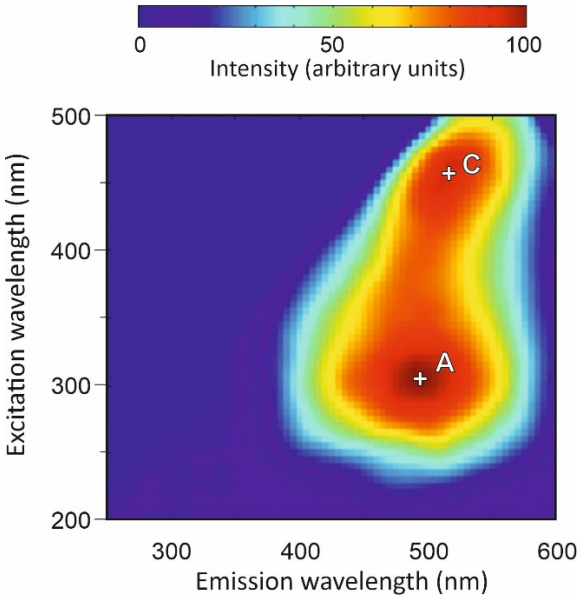

Fig. 1. Fluorescence excitation-emission matrix of the humic acid used in this study.

The 3D fluorescence signal of the HA used in our experiments is shown in Fig. 1. It indicated two peaks identified by their emission and excitation wavelengths at their maximum intensities. One (peak A) corresponds to fulvic-like molecules at (λ_{ex} = 305nm and λ_{em} = 495 nm) and the other (peak C) to humic-like molecules at (λ_{ex} = 460nm and λ_{em} = 520 nm) (Coble, 1996; Fellman, 2008; Ohno et Bro, 2006). The same spectrum was obtained at pH 4 and pH 9. It is typical of what was recorded elsewhere (Coble, 1996; Parlanti et al., 2002). The ability of natural organic matter, especially humic substances, to interact with metals is attributed to the presence of various functional groups such as amines, carboxyl, hydroxyl, phenolic or carbonyl. Metal ions or other complexing molecules are able to quench the fluorescence of organic ligands when they complex to these functional groups (Gauthier et al., 1986; Elkins and Donald, 2002; Provenzano et al., 2004). They can, in some cases, enhance the fluorescence intensity (Merdy et al., 2020 ; Manoharan et al., 2014).

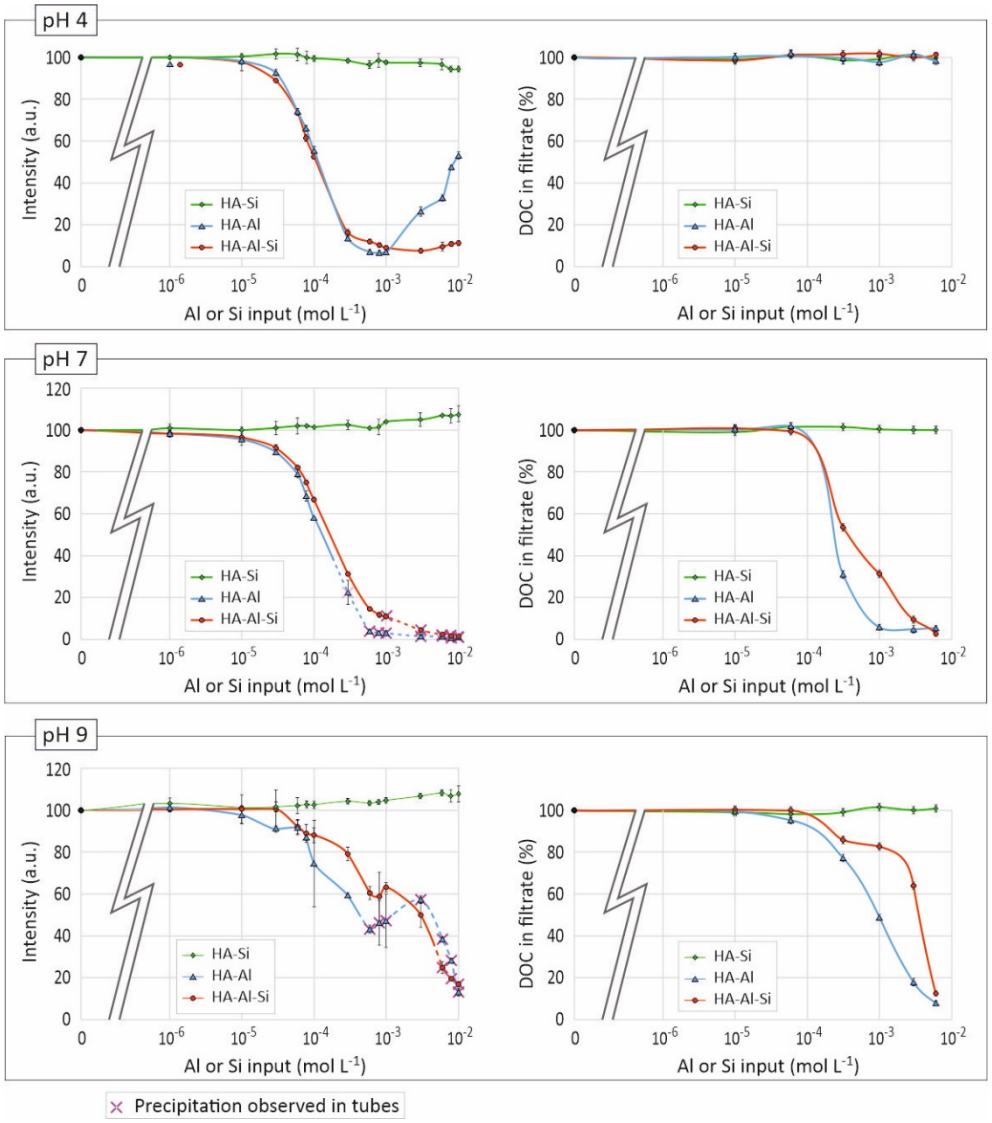

Fig. 2. Representation of the fluorescence intensity (no unit) of the different systems at different pHs as a function of the concentration of Si or Al (in mol L^{-1}). Fluorescence intensity and DOC % were normalized to their value in the pure HA solution (S15).

The left side of Fig. 2 shows the results of the quenching experiments, and the right side shows the measurement of organic carbon in the filtrates at each point of the experiment, which makes it possible to quantify any precipitation of organic matter. When carbon precipitation occurred, the fluorescence intensity Icalc was calculated assuming that the DOC remaining in solution had the same fluorescence properties as the DOC at the start of quenching:

$$I_{calc} = I_{obs} \frac{DOC_{init}}{DOC_{batch}}$$

Where I_{obs} and DOC_{batch} are the fluorescence intensity and the DOC concentration of the batch sample after filtration, respectively, and DOC_{init} is the DOC concentration at the beginning of the quenching experiment. The results are shown in Fig. 3.

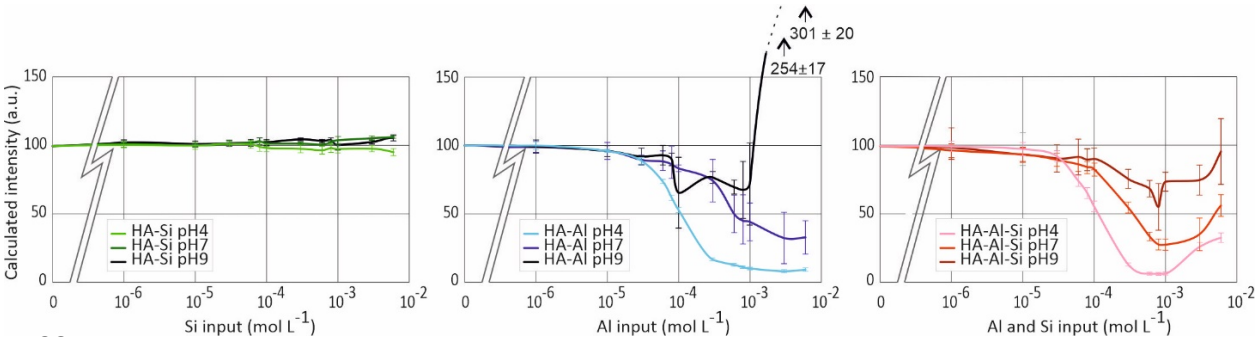

Fig. 3. Fluorescence intensity referred to the amount of DOC remaining in solution.

In the HA-Si system, the fluorescence intensity remained almost constant whatever the pH when the Si concentration increased to 10^{-4} mol L^{-1}. Starting from this concentration, there was a slight and reproducible fluorescence increase at pH 7 and 9 and a slight and reproducible decrease at pH4. No DOC precipitation occurred so these observations were not related to the removal of fluorophores from the solution. There is globally no strong fluorescence quenching or enhancement effect. This indicates negligible interactions between Si and HA at concentrations lower than 1.10^{-4} mol L^{-1}, which is consistent with the literature (Pokrovski and Schott, 1998), and slight direct interactions beyond this concentration under the experimental conditions. Although this was not visible in the experimental vials, precipitation of Si occurred when added Si was greater than 10^{-4} and 3 10^{-4} mol L^{-1} at pH 7 and 9, respectively (Fig. 4) (no data for pH 4). In the absence of Al, precipitation of Si likely occurred as a species whose solubility was intermediate between quartz and amorphous SiO_2 (Fig. 5), such as opal-a or opal-CT (Scheinost, 2005). According to Dietzel (2000), monosilicic acid is the largely dominant species of Si in solution up to pH 9.8 The possibility of condensation of monosilicic acid into polysilicic acid, which would have led to an increase in the binding capacity of dissolved Si, can therefore be ruled out for these experiments.

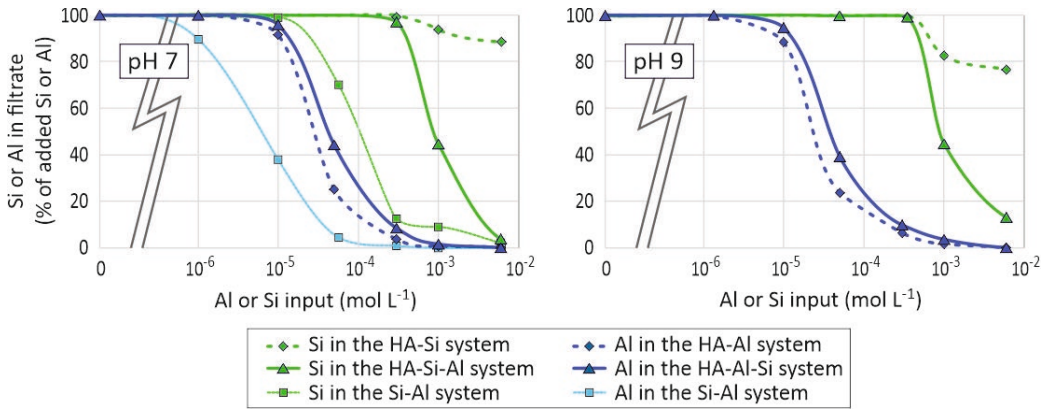

Fig. 4. Si or Al remaining in solution in the different systems at pH 7 and pH 9.

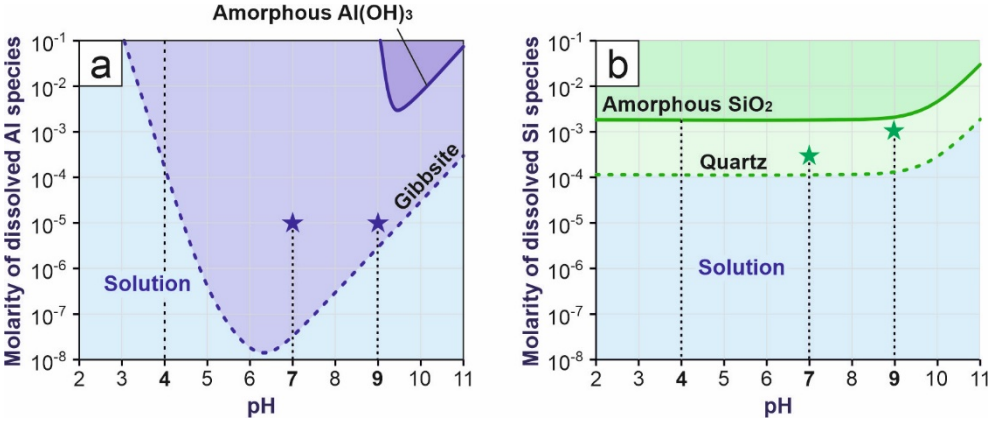

Fig. 5. Stability domain of amorphous $Al(OH)_3$ and gibbsite (a) and of amorphous SiO_2 and quartz (b). Blue and green stars indicate the Al or Si concentration at which precipitation began at the given pH in the HA-Al and HA-Si systems, respectively. Solubility products taken from the PHREEQC database (Johnson et al., 2000) and Furrer et al. (1991).

In the HA-Al system, an apparent fluorescence quenching was observed at any pH for Al input higher than 10^{-6} mol L^{-1}. DOC precipitation, however, occurred at Al input greater than 10^{-4} and 10^{-5} mol L^{-1} at pH 7 and 9, respectively (Fig. 2). Such precipitation was expected given the flocculating power on DOC by Al species in solution at sufficiently high concentration, as demonstrated by several studies (Nierop et al., 2002; Mason et al., 2000; Sadrnourmohamadi and Gorczyca, 2015), or by DOC adsorption on newly precipitated Al hydroxides (Heckman et al., 2013). Aluminium precipitation, however, occurred at Al input greater than 3.10^{-6} mol L^{-1} at pH 7 and 9 (Fig. 3), when no DOC precipitation was observed between 3.10^{-6} and 3.10^{-5} mol L^{-1}, so that HA adsorption on Al hydroxides was not the main process. In the absence of Si, precipitation of Al likely occurred as species whose solubility was intermediate between gibbsite and amorphous $Al(OH)_3$ (Fig. 5), such as Al_{13} gel (Jolivet, 2000).

After correction of the precipitated DOC, fluorescence quenching was confirmed at pH 4 and 7 over the entire concentration range (Fig. 3). At pH 9, the fluorescence quenching observed at Al input of between 10^{-5} and 10^{-3} mol L^{-1} was followed by a fluorescence enhancement at greater Al input. The fluorescence enhancement effect on natural organic matter complexed with Al had already been observed (Blaser et al., 1999; Sharpless and McGown, 1999; Elkins et al., 2002). Elkins et al. (2002) considered Al to be unique compared to other metal ions such as Cu, Co, Mn, Pb, which have a propensity to quench the fluorescence; Al would be different due to its high charge density. Other studies showed a quenching phenomenon of natural organic matter upon Al ion addition, such as Shotyk and Sposito (1988) on leaf litter aqueous extract at λ_{ex} = 440 nm and λ_{em} = 525 nm at pH = 4.0, 4.5, and 5.0. More recent studies tried to identify the processes responsible for quenching or enhancement of the fluorescence signal, such as that of Yan et al. (2013). If the quenching of fulvic acid signals was dominating at higher emission wavelengths and increasing total Fe(III) concentrations, the pattern observed with Al(III) was much more complex with both quenching and enhancement phenomena observed in different areas of the spectra. Basically, at low concentrations, the authors mentioned that the interactions took place with phenolic groups of the fulvic acid, and then weakly binding carboxylic groups. After saturation of the complexing sites, metallic ions keep interacting with fulvic acids through non-specific Donnan gel electrostatic

interactions. The specific pattern observed for Al(III) ions at pH 6 was not fully understood by these authors and could be explained, according to them, by discrete subsets of natural organic matter fluorophores. This last assumption could apply here, where the transition from quenching to enhancement when added Al increased could be explained by the precipitation of a subset of fluorophores, the fluorophores remaining in solution having higher quantum yields. Greater ionic strength when Al input increased may also have resulted in Al decomplexation from fluorophores. Because of the precipitation of both Al and organic matter, however, the verification of this hypothesis would require dedicated studies.

In the HA-Si-Al system, the evolution of fluorescence is close to that of the HA-Al system, but the DOC precipitation is lower than in the latter for Si or Al inputs between 10^{-4} and 8 10^{-3} mol L^{-1}. There was no fluorescence enhancement, but it was observed after correction of the precipitated DOC that the quenching was maximum for Si or Al inputs around 10^{-3} mol L^{-1} and decreased when metal concentrations increased. The presence of Si changed the behavior of the system compared to the presence of Al alone. For metal input greater than 8 10^{-4} mol L^{-1}, both quenching (at pH 4 and 7) and enhancement (at pH 9) became less intense in the HA-Si-Al system, unlike what was observed in the HA-Al system.

In order to evaluate the role of HA in the precipitation of Al and Si, we measured the Si and Al remaining in solution in a Si-Al system without HA at pH 7, using the same batch protocol as for the quenching measurements; the results are shown in Fig. 4. It can be seen that with increasing inputs of Si and Al, the presence of HA delayed precipitation of both Al and Si. This can be explained by the formation of HA-Al complexes, which delayed the precipitation of Al hydroxides and aluminosilicates. However, precipitation of DOC (Fig. 2) and Al (Fig. 4) was lower in the HA-Si-Al system than in the HA-Al system for amounts of added metal less than 8 10^{-3} mol L^{-1}, at pH 7 as well as at pH 9. The presence of Si therefore favored the maintenance of both DOC and Al in solution. Consequently, the supposition of DOC and Al removal by precipitation of minerals and subsequent HA adsorption cannot explain the experimental observation, and the process of DOC flocculation by Al^{3+} species is at least slowed down by dissolved silicon.

At this stage of the study, our hypothesis to explain our data is the formation of a ternary complex between HA, Al and Si. At pH of around 5.5 to 7.5, Al^{3+} in its octahedral first hydration shell is more likely than Si^{4+} in its tetrahedral first hydration shell to form an inner sphere complex with a reactive nucleophilic site of the NOM (Jolivet et al., 2000). Indeed, Al^{3+} has a much higher affinity than Si^{4+} with HA. It is therefore very likely that Al play facts as a bridge between NOM and a Si species, with an Al-O-Si bond.

3.2. IR spectroscopy

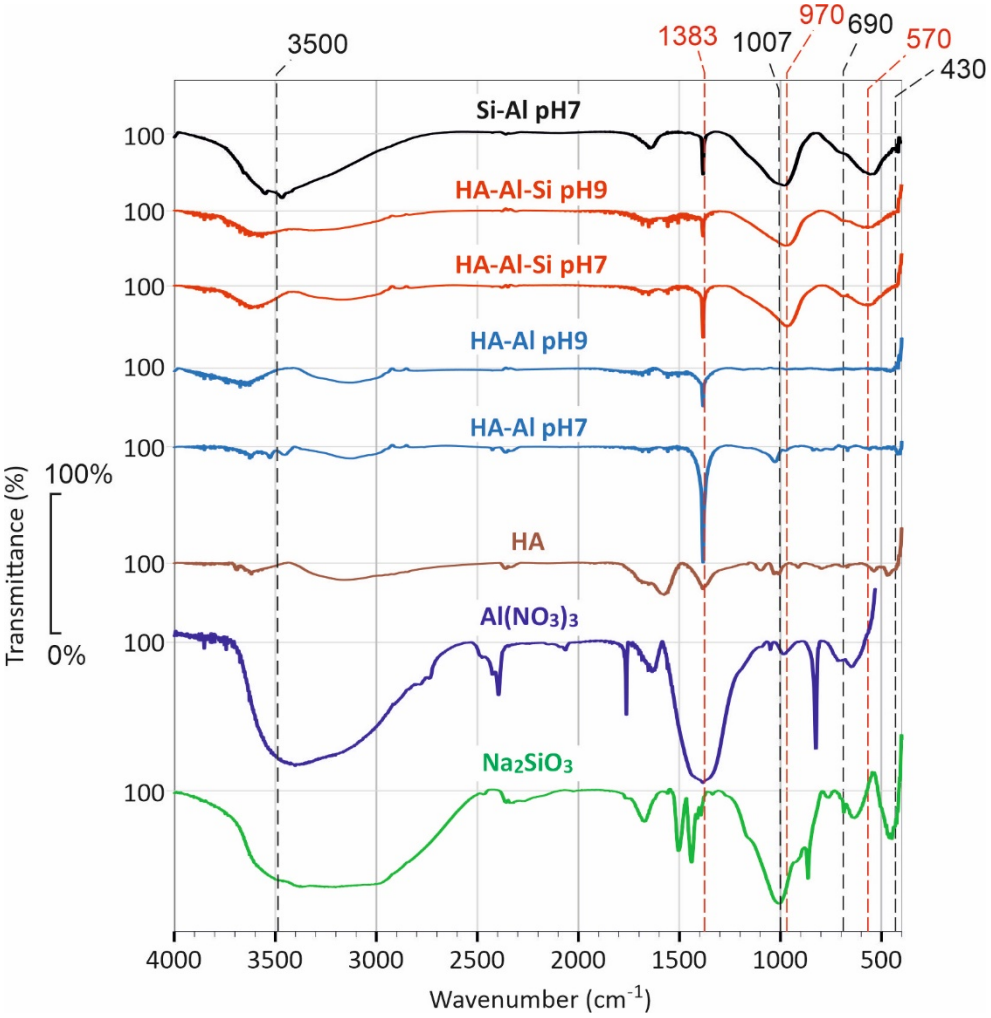

Fig. 6. IR spectra of the solid phases collected on the membrane filters in the different systems.

The IR spectra of Na_2SiO_3 and of the different solids precipitated from batches are given in Fig. 6. The IR spectrum of Na_2SiO_3 was similar to that obtained by Yahya et al. (2015). The Si-O vibration frequency can be seen at 1007 cm^{-1} (Halasz et al., 2007). The broad band around 3000-3800 cm^{-1} observed in most spectra is characteristic of an OH bond elongation in Si-OH, Al-OH and water. The 1387 cm^{-1} frequency observed where Al was present corresponds to N-O bonds in NO_3^- (Kloprogge, 2001). The two bands at 740 and 830 cm^{-1} correspond to deformation modes of nitrate (Ruiz Madronero and Rodriguez Paéz, 2010).

In the HA spectrum, the C=O vibration band from the carboxylic functional group appeared at 1700 cm^{-1} and 1400 cm^{-1} where the –COOH group is partially converted into its salt form $–COO^-$. A definite assignment of bands around 1600 cm^{-1} is still unsure: according to Stevenson (1971), it could be assigned to aromatic C=C stretch vibration, H-bonded C=O of quinones or H-bonded and conjugated ketones of the type β-diketones (-CO-CH_2-CO-). The C-O stretch of alcohol, polysaccharide-like substances and/or aliphatic ether appeared at 1000 and 1100 cm^{-1} (Rodriguez, 2011; Stevenson, 1971). It should be noted that C-O stretching and O-H deformation of carboxylic groups could also explain the absorption near 1100 or 1200 cm^{-1}.

The two bands of HA at 1600 and 1700 cm^{-1} disappeared almost entirely after Al was added to HA. The same observation can be made for the 1100 cm^{-1} band.

These ascertainments seem to indicate that Al was binding to carboxylic groups but also to alcohol and ether groups of HA.

We have to be careful with the band at 1650 cm^{-1} present in Na_2SiO_3 and $Al(NO_3)_3$ since it could be attributed to deformation vibration of the O-H bond from water (Myronyuk et al., 2016).

The HA-Si-Al ternary system IR spectrum was similar to that obtained by Rouff et al. (2012) on the same type of system. Interestingly, the HA-Si-Al and HA-Al spectra exhibited a clear difference: a band at 1007 cm^{-1} was observed in the HA-Al system while another one was observed at 970 cm^{-1} in the HA-Si-Al system, showing that the complexes HA-Si-Al and HA-Al were not the same, which strongly suggests that Si takes part in the ternary complex. In fact, the band at 970 cm^{-1} was attributed to the elongation of the Si-O bond and the band at 1007 cm^{-1} could supposedly be associated with Al-O vibration, with oxygen coming from HA.

The band from 400 to 800 cm^{-1} comes from the elongations of the Si-O-Al and Si-O-Si stretching bonds. The 630 cm^{-1} of the Al-O band (Nakamato, 1962) observed for the Na_2SiO_3 sample shifted towards 570 cm^{-1} in the Si-Al and HA-Si-Al systems. This shift could indicate that Al complexed to an aluminosilicate oxygen or an HA oxygen. Additionally, this band is indicative of an imogolite-like structure observed in natural allophane and imogolite, with a peak at 570 cm^{-1} and a shoulder at 690 cm^{-1} and 430 cm^{-1}. This pattern is the signature of the Si and Al association.

As a conclusion, the IR spectra indicated Al with Si association on one hand and HA with Al association on the other. The differences between HA-Al and HA-Si-Al at 1000cm^{-1} and 970 cm^{-1} suggest the presence of an HA-Al-Si ternary complex.

3.3. Colloid size distribution

The colloid size distribution was determined by Nano Tracking Analysis on solutions with 120 mg L^{-1} HA and 10^{-3} mol L^{-1} of Si and/or Al. The size distributions are given in Fig. 7, particle scattering intensities are given in Fig. 8 and statistics of the size distribution are given in Table 2.

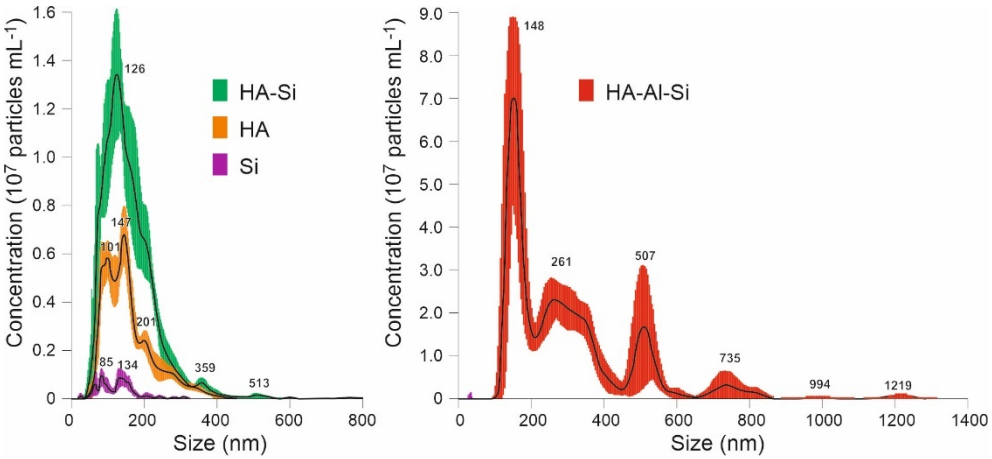

Fig. 7. Particles size distribution obtained by Nano Tracking Analysis. Error bars indicate ±1 standard error of the mean.

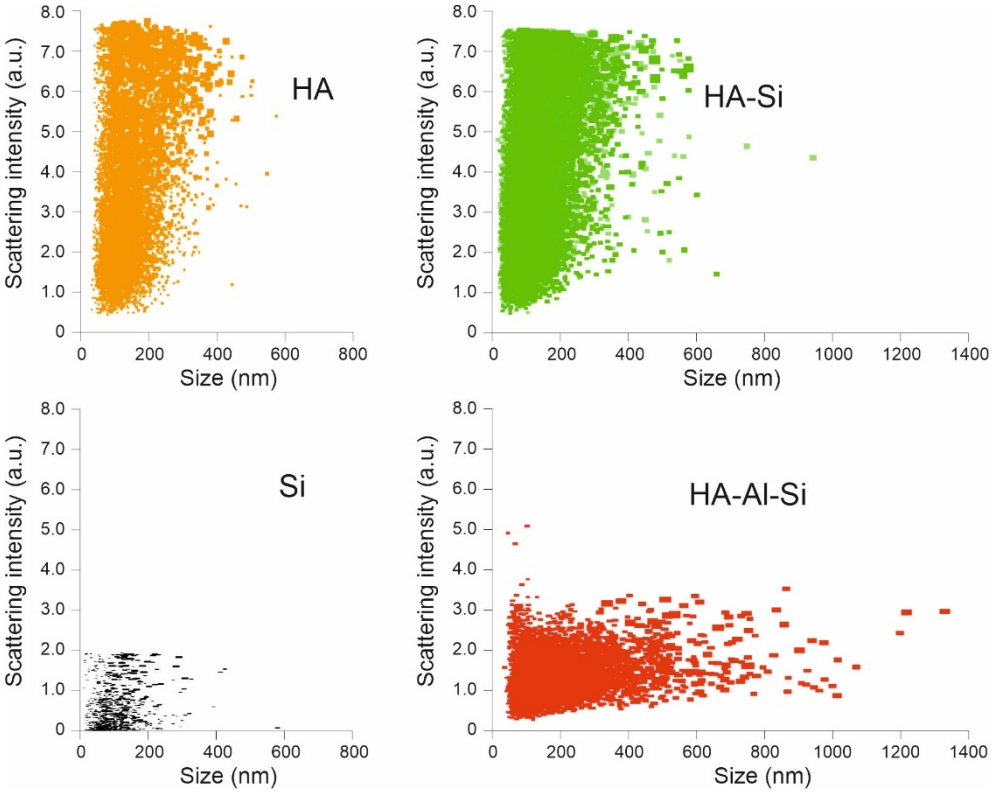

Fig. 8. Particle scattering intensity represented as a function of size distribution in the systems HA, HA-Si, Si and HA-Al-Si.

Table 2
Statistics of the size distribution.

Solution	Concentration of total particles (particles mL^{-1})	Mean (nm)	Mode (nm)
Si	$7.9\ 10^{7} \pm 0.8\ 10^{7}$	134 ± 2	116 ± 17
HA	$7.9\ 10^{8} \pm 3.2\ 10^{8}$	158 ± 3	124 ± 12
HA-Si	$1.7\ 10^{9} \pm 0.07\ 10^{9}$	158 ± 3	119 ± 8
HA-Al-Si	$9.1\ 10^{9} \pm 0.3\ 10^{9}$	289 ± 45	213 ± 72

The Si solution showed a small concentration of small colloidal particles, which may be silica precipitates. The HA solution showed particles in the same size range but with a concentration one order of magnitude higher. Comparison of the size distribution shows that when Si was added to HA, the size of the particles did not change significantly but their number increased. There was, therefore, very probably an interaction between dissolved Si and HA that favored the formation of small colloids. This assumption is supported by the fact that the small particles of very low scattering intensity which were observed in the Si solution (Fig. 8) were no longer observed in the HA-Si solution. This can be explained because dissolved Si, interacting with HA, was no longer available for silica precipitation.

The HA-Al-Si solution showed particles larger and more numerous than in the HA-Si solution, which is consistent with the results obtained in fluorescence spectroscopy. As for the HA-Si solution, the small particles of very low scattering

intensity characteristic of the Si solution were not observed. The particle scattering intensity in the HA-Al-Si solution was lower than in the HA and the HA-Si solution. This indicates different form and/or structure factors, which remain to be determined.

Silica scattered little light compared to HA. It was therefore differentiable when it was isolated. On the other hand, whether or not it was in the presence of Si, the light scattering of HA remained the same, again confirming the absence of interactions or the little interaction between HA and Si. In contrast, signals specific to isolated silica particles no longer existed in the ternary system, suggesting that Si was involved in complexes.

3.4. Solid-state NMR of ^{29}Si

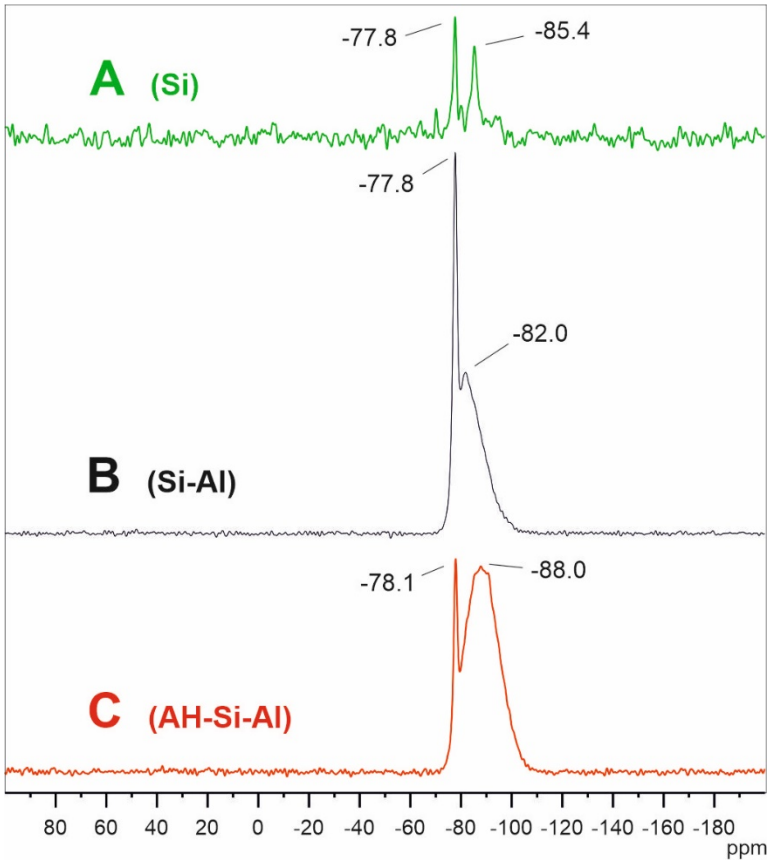

Fig. 9. ^{29}Si Solid State NMR spectra of the particles precipitated in the batch solutions at pH7 (HA 120 mg L^{-1}, Si and Al 10^{-2} mol L^{-1})

Fig. 9 A shows the typical ^{29}Si NMR signal of the SiO_3 compound at -77 ppm and a narrow signal at -85 ppm, indicating a partial condensation of a Si-O-Si group (Jones et al., 2005). Fig. 9 B shows, in addition to the signal of free SiO_3, a broad signal at -82 ppm characteristic of a Si-O-Al bond (2). The addition of HA (Fig. 9 C) causes a shift in the complexation signal of the Si-O-Al group probably due to the interaction with the organic substance. It should be noted that the signal for the Si-O-Al complex has a higher intensity than in the case of aluminium alone. Since the ^{29}Si technique used has been optimized for a semi-quantitative regime, it can be concluded that the presence of HA favored the formation of the Si-O-Al bond compared to the Si-Al system, which supports the assumption given above. The data acquired does not, however, allow the size of the compounds complexed

513 with HA to be determined. They may be complexes of reduced size with one Al
514 and one Si only, or nanocolloids of aluminosilicates.
515 Liu et al. (2011) indirectly evidenced Fe-bridged As−Fe-DOM complexes, which
516 are likely due to the same type of interaction as described here. Dupuis et al.
517 (1982), studying the effect of fulvic acid on Si-Mg colloids, obtained results
518 suggesting the presence of FA-Mg-Si complexes. More broadly, this type of
519 interaction is likely to exist with other metals than Al, such as Fe or Mn, and other
520 metalloids than Si, such as As or Ge.
521
522 *3.5. Implications in the soil-water-plant continuum*
523
524 The presence of HA-Al-Si complexes suggested by our study may appear, at a
525 first glance, to contradict previous studies, such as those of Viers et al. (1997,
526 2000). These authors studied rivers in Cameroon and concluded that Si does not
527 complex with humic substances because (1) there was no correlation between
528 dissolved Si (DSi) and dissolved organic carbon (DOC) when a correlation was
529 observed between DOC and dissolved Al (DAl), and (2) after separation of
530 dissolved and colloidal fractions by ultrafiltration, 100% of Al was found in the
531 colloidal fraction while Si was predominantly in the dissolved fraction. We argue
532 that these observations are not demonstrative, given the high level of DSi (8-18
533 mg L^{-1}) compared to DAl (<0.2 mg L^{-1}) in the studied rivers. If only a minor fraction
534 of Si was complexed with HA and Al, it has no weight in the correlation and is
535 included in the small amount of Si observed in the colloidal fraction.
536 On the other hand, the presence of HA-Al-Si complexes suggested by our study
537 is in agreement with the assumptions put forward to interpret the experiments of
538 Merdy et al. (2021). These authors showed, in laboratory column percolations of
539 podzolic horizons, that certain types of organic matter can promote the transfer
540 of Al and DOM through kaolinitic materials and presume the existence of DOM-Al-
541 Si complexes. There is also a parallel between our results, in which Si in solution
542 binds to organic matter via a bridging Al, and earlier results from Bartoli (1985),
543 which presented compelling evidence that an organic matter, alanine, binds to a
544 silica surface via a bridging Al. This type of complex certainly plays a role in soil
545 processes other than mineral-solution relationships. Li et al. (2020) showed, for
546 example, that such complexes are probably involved in phytoliths cycling, and
547 therefore Si cycling, in soils.
548 The identification of DOM-Al-Si complexes may also have some impact on the
549 knowledge of Al-Si interactions in plant biology. Aluminum is recognized as toxic
550 to plants, but Si has been proven to alleviate its deleterious effect (Hodson and
551 Evans, 2020). The mechanisms are not fully elucidated but one hypothesis is that
552 Al and Si, which have a strong affinity in soil solution, may combined to form
553 insoluble hydroxyaluminosilicates (HAS) (Beardmore et al., 2016). Therefore, the
554 formation of HAS may have the ability to attenuate the root uptake of Al. As
555 Hodson and Evans (2020) mentioned, equilibrium with respect to HAS is assumed,
556 but it may not be the case. Our results suggest another Al sequestration
557 mechanism, that does not require equilibrium with HAS: the formation of DOM-
558 Al-Si complexes. Such complexes can, of course, lead to the formation of HAS if
559 the DOM is destroyed by microorganisms. However, more research is needed to
560 explore this hypothesis.
561

4. Conclusion

Until now, interaction between Si and organic matter was considered non-existent or very weak; our fluorescence experiments confirmed that HA-Si interactions exist but are weak. Through several complementary techniques, however, we have shown that stronger HA-Si interactions exist but in the presence of an intermediate ion such as Al^{3+} by the formation of a ternary complex HA-Al-Si with bridging Al and an Al-O-Si bond. Such DOM-Al-Si complexes can play an important role in pedogenesis wherever dissolved organic matter (DOM) is abundant, such as in the surface horizons of most soils or horizons in which podzolic processes occur. The presence of Si significantly promotes the maintenance of both Al and DOM in solution, which is likely to modify the result or the kinetics of the processes of dissolution/precipitation of minerals, therefore of pedogenesis.

These results pave the way for further studies, both at the molecular level to better specify the structure of the complexes, and at the macroscopic scale to determine their equilibrium and kinetic constants. In addition, the type of interaction shown here with Al and Si probably also exists with other metals, such as Fe or Mn, and other metalloids, such as As.

Acknowledgments

The authors thank Cyril Neytar for his participation in the laboratory work.

Funding

This work was funded by the French ANR program BioSiSol ANR-14-CE01-0002.

References

Bartoli F., 1985. Crystallochemistry and surface properties of biogenic opal. J. Soil Sci. 36, 335–350. doi:10.1111/j.1365-2389.1985.tb00340.x

Beardmore, J., Lopez, X., Mujika, J.I., Exley, C., 2016. What is the mechanism of formation of hydroxyaluminosilicates? Sci. Rep. 6, 30913. https://doi.org/10.1038/srep30913.

Bennett, P.C., 1991. Quartz dissolution in organic-rich aqueous systems. Geochim. Cosmochim. Acta 55, 1781-1797. https://doi.org/10.1016/0016-7037(91)90023-X.

Bennett, P.C., Siegel, D.I., Hill, B.M., Glaser, P.H., 1991. Fate of silicate minerals in a peat bog. Geology 19, 328-331. https://doi.org/10.1130/0091-7613(1991)019<0328:FOSMIA>2.3.CO;2

Blaser, P., Heim, A., Luster, J., 1999. Total luminescence spectroscopy of NOM-typing samples and their aluminium complexes. Environ. Int. 25, 285–293. https://doi.org/10.1016/S0160-4120(98)00106-8.

Bro, R., 1997. PARAFAC. Tutorial and applications. Chemom. Intell. Lab. Sys. 38, 149-171. https://doi.org/10.1016/S0169-7439(97)00032-4.

Cha, J.N., Shimizu, K., Zhou, Y., Christiansen, S.C., Chmelka, B.F., Stucky, G.D., Morse, D.E., 1999. Silicatein filaments and subunits from a marine sponge

608 direct the polymerization of silica and silicones in vitro. PNAS, 96, 361–365.
609 http://www.jstor.org/stable/46816
610 Coble, P.G., 1996. Characterization of marine and terrestrial DOM in seawater
611 using excitation-emission matrix spectroscopy. Mar. Chem., 51, 325-346.
612 https://doi.org/10.1016/0304-4203(95)00062-3.
613 Cook, R.L., Langford, C.H., Yamdagni, R., Preston, C.M., 1996. A modified cross-
614 polarization magic angle spinning ^{13}C NMR procedure for the study of humic
615 materials. Anal. Chem. 68, 3979– 3986. https://doi.org/10.1021/ac960403a.
616 Cornelis, J.T., Delvaux, B., Georg, R.B., Lucas, Y., Ranger, J., Opfergelt, S. 2011.
617 Tracing the origin of dissolved silicon transferred from various soil-plant
618 systems towards rivers: a review. Biogeosci. 8, 89-112.
619 https://doi.org/10.5194/bg-8-89-2011.
620 Dietzel, M., 2000. Dissolution of silicates and the stability of polysilicic acid.
621 Geochim. Cosmochim. Acta 64, 3275-3281. https://doi.org/10.1016/S0016-
622 7037(00)00426-9
623 Dupuis, Th., Jambu, P., Dupuis, J., 1982. Etude expérimentale de l'action des
624 acides fulviques sur les gels silico-magnésiens et les silicates magnésiens. Sci.
625 Sol 4, 241-252.
626 Elkins, K.M., Nelson, D.J., 2002. Spectroscopic approaches to the study of the
627 interaction of aluminum with humic substances. Coordin. Chem. Rev. 228, 205-
628 225. https://doi.org/10.1016/S0010-8545(02)00040-1.
629 Fellman, J.B., D'Amore, D.V., Hood, E., Boone, R.D., 2008. Fluorescence
630 characteristics and biodegradability of dissolved organic matter in forest and
631 wetland soils from coastal temperate watersheds in southeast Alaska.
632 Biogeochem. 88, 169-184. https://doi.org/10.1007/s10533-008-9203-x.
633 Furrer, G., Ludwig, C., Schindler, P., 1991. On the chemistry of the Keggin Al_{13}
634 polymer: I. Acid-base properties. J. Coll. Interf. Sci. 149, 56-67.
635 https://doi.org/10.1016/0021-9797(92)90391-X.
636 Gauthier, T.D., Shane, E.C., Guerin, W.F., Seitz W.R., Grant C.L., 1986.
637 Fluorescence quenching method for determining equilibrium constants for
638 polycyclic aromatic hydrocarbons binding to dissolved humic materials.
639 Environ. Sci. Technol. 20, 1162-1166.
640 Gerbaud, G., Ziarelli, F., Caldarelli, S., 2003. Increasing the robustness of
641 heteronuclear decoupling in magic-angle sample spinning solid-state NMR,
642 Chem. Phys. Lett. 377, 1-5. https://doi.org/10.1016/S0009-2614(03)01056-X.
643 Greiser, S., Gluth, G.J.G., Sturmb, P., Jäger, C., 2018. $^{29}Si\{^{27}Al\}$, $^{27}Al\{^{29}Si\}$ and
644 $^{27}Al\{^{1}H\}$ double-resonance NMR spectroscopy study of cementitious sodium
645 aluminosilicate gels (geopolymers) and gel-zeolite composites. RSC Advances 7,
646 4164 – 4171. https://doi.org/10.1039/C8RA09246J.
647 Halasz, I., Agarwal, M., Li, R., Miller, N., 2007. Vibrational spectra and dissociation
648 of aqueous Na_2SiO_3 solutions. Catal. Lett. 117, 34-42.
649 https://doi.org/10.1007/s10562-007-9141-6.
650 Heckman, K., Grandy, A.S., Gao, X., Keiluweit, M., Wickings, K., Carpenter, K.,
651 Chorover, J., Rasmussen, C., 2013. Sorptive fractionation of organic matter and
652 formation of organo-hydroxy-aluminum complexes during litter
653 biodegradation in the presence of gibbsite. Geoch. Cosmoch. Acta 121, 667-
654 683. https://doi.org/10.1016/j.gca.2013.07.043.
655 Hodson, M.J., Evans, D.E., 2020. Aluminium–silicon interactions in higher plants:
656 an update. J. Exp. Bot. 71, 6719–6729. https://doi.org/10.1093/jxb/eraa024.

Inanaga, S., Okasaka, A., Tanaka, S., 1995. Does silicon exist in association with organic compounds in rice plant? Soil Sci. Plant Nutr. 41, 111-117. https://doi.org/10.1080/00380768.1995.10419564.

Inanaga, S., Okasaka, A., 1995. Calcium and silicon binding compounds in cell wall of rice shoots. Soil Sci. Plant Nutr. 41, 103-110. https://doi.org/10.1080/00380768.1995.10419563.

Johnson, J., Anderson, F., Parkhurst, D.L., 2000. Database thermo.com.V8.R6.230, Rev 1.11. Lawrence Livermore National Laboratory, Livermore, California.

Jolivet, J.P., Henry, M., Livage, J., 2000. Metal oxide chemistry and synthesis : from solution to solid state. John Willey, Chichester.

Jones, L.H.P, Handreck, K.A.,1967. Silica in soils, plants and animals. Adv. Agron. 19, 107-149. https://doi.org/10.1016/S0065-2113(08)60734-8.

Jones, A.R., Winter, R., Greaves, G.N., Smith, I.H., 2005. ^{23}Na, ^{29}Si, and ^{13}C MAS NMR investigation of glass-forming reactions between Na_2CO_3 and SiO_2. J. Phys. Chem. B 109, 23154-23161. https://doi.org/10.1021/jp053953y.

Kambalina, M., Mazurova, I., Skvortsova, L., Guseva, N., An, V., 2014. Study of aqueous chemical forms of silicon in organic-rich waters. Procedia Chem. 10, 36-42. https://doi.org/10.1016/j.proche.2014.10.008.

Kan, S.B.J, Lewis, R.D., Chen, K., Arnold, F.H., 2016. Directed evolution of cytochrome c for carbon-silicon bond formation: bringing silicon to life. Science 354, 1048-1051. https://doi.org/10.1126/science.aah6219.

Keller, C., Guntzer, F., Barboni, D., Labreuche, J., Meunier, J. D., 2012. Impact of agriculture on the Si biogeochemical cycle: input from phytolith studies. C. R. Geosci. 344, 739-746. https://doi.org/10.1016/j.crte.2012.10.004.

Kennedy, J.A., Powell, H.K.J., 1986. Colorimetric determination of aluminium (III) with chrome azurol S and the reactivity of hydrolysed aluminium species. Anal. Chim. Acta 184, 329-333. https://doi.org/10.1016/S0003-2670(00)86501-0.

Kloprogge, J.T., Ruan, H., Frost, R.L., 2001. Near-infrared spectroscopic study of basic aluminum sulfate and nitrate. J. Mat. Sci. 36, 603–607. https://doi.org/10.1023/A:1004860118470.

Kolesnikov, M.P., Gins, V.K., 2001. Forms of silicon in medicinal plants. Appl. Biochem. Microbiol. 37, 524-527. https://doi.org/10.1023/A:1010262527643.

Larina, L.I., 2021. Chapter One - Organosilicon azoles: Structure, silylotropy and NMR spectroscopy, in: Scriven, E.F.V., Ramsden, C.A. (Eds.), Advances in Heterocyclic Chemistry Volume 133, Academic Press, London, pp. 1-63. https://doi.org/10.1016/bs.aihch.2019.08.001.

Li, J., Zheng, L., Wang, S-L., Wu, Z., Wu, W., Niazi, N.K., Shaheen, S.M., Rinklebe, J., Bolan, N., Ok, Y.S., Wang, H. (2019). Sorption mechanisms of lead on silicon-rich biochar in aqueous solution: Spectroscopic investigation. Sci. Tot. Env. 672, 572-582.

Lindsay, W.L., Walthall, P.M., 2020. The solubility of aluminum in soils, in: Sposito, G. (Ed.), The environmental chemistry of aluminum, CRC Press, pp. 333-361.

Liu, G., Fernandez, A., Cai, Y., 2011. Complexation of arsenite with humic acid in the presence of ferric iron. Environ. Sci. Technol. 45, 3210-3216. https://doi.org/10.1021/es102931p.

Lucas, Y., Luizao, F.J., Chauvel, A., Rouiller, J., Nahon, D., 1993. The relation between biological activity of the rainforest and mineral composition of the soils. Science 260, 521-523. https://doi.org/10.1126/science.260.5107.521.

Luster, J., Lloyd, T., Sposito, G., Fry, I.V., 1996. Multi-wavelength molecular fluorescence spectrometry for quantitative characterization of copper(II) and

708 aluminum(III) complexation by dissolved organic matter. Environ. Sci. Technol.
709 30: 1565-1574. https://doi.org/10.1021/es950542u.
710 Ma, J.F., Yamaji, N., 2015. A cooperative system of silicon transport in plants.
711 Trends Plant Sci. 20, 435-442. https://doi.org/10.1016/j.tplants.2015.04.007
712 Ma, C., Ci, K., Zhu, J., Sun, Z., Liu, Z., Li, X., Zhu, Y., Tang, C., Wang, P., Liu, Z.
713 (2021).Impacts of exogenous mineral silicon on cadmium migration and
714 transformation in the soil-rice system and on soil health. Sci. Tot. Env. 759,
715 143501. https://doi.org/10.1016/j.scitotenv.2020.143501
716 Manoharan, V., Ravindran, A., Anjali, C.H., 2014. Mechanistic insights into
717 interaction of humic acid with silver nanoparticles. Cell Biochem. Biophys. 68,
718 127–131. https://doi.org/10.1007/s12013-013-9699-0.
719 Masion, A., Vilgé-Ritter, A., Rose, J., Stone, W.E.E., Teppen, B.J., Rybacki, D.,
720 Bottero, J.Y., 2000. Coagulation-flocculation of natural organic matter with Al
721 salts: speciation and structure of the aggregates. Environ. Sci. Technol. 34,
722 3242-3246. https://doi.org/10.1021/es9911418
723 Matychenkov, I.V., Khomyakov, D.M., Pakhnenko, E.P., Bocharnikova, E.A.,
724 Matychenkof, V.V., 2016. Mobile Si-rich compounds in the soil–plant system
725 and methods for their determination. Moscow Univ. Soil Sci. Bull. 71, 120–128.
726 https://doi.org/10.3103/S0147687416030054
727 Merdy, P., Neytard, C., Meunier, J.D., Lucas, Y., 2020. PDMPO: a specific silicon or
728 silica, pH sensitive fluorescent probe? RSC Advances 10, 31003-31011.
729 https://doi.org/10.1039/D0RA05108J].
730 Merdy, P., Lucas, Y., Coulomb, B., Melfi, A.J., Montes, C.R., 2021. Soil organic
731 carbon mobility in equatorial podzols: soil column experiments. Soil 7, 585-
732 594. https://doi.org/10.5194/soil-7-585-2021
733 Mitani, N., Ma, J.F., Iwashita, T., 2005. Identification of the silicon form in xylem
734 sap of rice (Oryza sativa L.). Plant Cell Physiol. 46, 279–283.
735 https://doi.org/10.1093/pcp/pci018.
736 Myronyuk, I.F., Mandzyuk, V.I. , Sachko, V.M. , Gun'ko, V.M., 2016. Structural and
737 morphological features of disperse alumina synthesized using aluminum
738 nitrate nonahydrate. Nanoscale Res. Lett. 11,153.
739 https://doi.org/10.1186/s11671-016-1366-0.
740 Nakamoto, K., 1962. Infrared spectra of inorganic and coordination compounds,
741 John Wiley & Inc., New York - London.
742 Nierop, K.G.J.J., Jansen, B., Verstraten, J.M., 2002. Dissolved organic matter,
743 aluminium and iron interactions: precipitation induced by metal/carbon ratio,
744 pH and competition. Sci. Tot. Env. 300, 201-211.
745 https://doi.org/10.1016/S0048-9697(02)00254-1.
746 Ohman, L.O., Nordin, A., Sedeh, F.I., Sjöberg, S., 1991. Equilibrium and structural
747 studies of silicon(IV) and aluminium(III) in aqueous solution. 28. Formation of
748 soluble silicic acid-ligand complexes as studied by potentiometric and solubility
749 measurements. Acta Chem. Scand. 45, 335-341.
750 Ohno, T., Bro, R., 2006. Dissolved organic matter characterization using multiway
751 spectral decomposition of fluorescence landscapes. Soil Sci. Soc. Am. J. 70,
752 2028-2037. https://doi.org/10.2136/sssaj2006.0005.
753 Otzen, D., 2012. The role of proteins in biosilicification. Scientifica, 2012, ID
754 867562. https://doi.org/10.6064/2012/867562
755 Parlanti, E., Morin, B., Vacher, L., 2002. Combined 3D-spectrofluorimetry, high
756 performance liquid chromatography and capillary electrophoresis for the
757 characterization of dissolved organic matter in natural waters. Org. Geochem.
758 33, 221–236.

759 Peersen, O.B., Wu, X., Kustanovich, I., Smith, S.O., 1993. Variable-amplitude cross-
760 polarization MAS NMR. J. Magn. Reson. 104, 334–339.
761 https://doi.org/10.1006/jmra.1993.1231.
762 Perry, C.C., 2015. An overview of silica in biology: its chemistry and recent
763 technological advances, in: Müller, W.E.G., Grachev, M.A. (Eds.), Biosilica in
764 Evolution, Morphogenesis, and Nanobiotechnology, Progress in Molecular and
765 Subcellular Biology, Marine Molecular Biotechnology 47, 295-313. DOI:
766 10.1007/978-3-540-88552-8,
767 Pokrovski, G.S., Schott, J., 1998. Experimental study of the complexation of silicon
768 and germanium with aqueous organic species: implications for germanium and
769 silicon transport and Ge/Si ratio in natural waters. Geochim. Cosmochim Acta
770 62, 3413-3428. https://doi.org/10.1016/S0016-7037(98)00249-X.
771 Poulson, S.R., Drever, J.I., Stillings, L.L.,1997. Aqueous Si-oxalate complexing,
772 oxalate adsorption onto quartz, and the effect of oxalate upon quartz
773 dissolution rates. Chem. Geol. 140, 1-7. https://doi.org/10.1016/S0009-
774 2541(96)00177-5
775 Provenzan, M.R., D'Orazio, V., Jerzykiewicz, M., Senesi, N., 2004. Fluorescence
776 behaviour of Zn and Ni complexes of humic acids from different sources .
777 Chemosphere 55, 885-892.
778 https://doi.org/10.1016/j.chemosphere.2003.11.040.
779 Rouff, A.A., Phillips, B.L., Cochiara, S.G., Nagy, K.L., 2012. The Effect of dissolved
780 humic acids on aluminosilicate formation and associated carbon sequestration.
781 Appl. Env. Soil Sci. 2012, ID 430354. https://doi.org/10.1155/2012/430354.
782 Ruiz Madroñero, C.V., Rodríguez Paéz, J.E., 2010. Sodium aluminates obtained
783 from the $Al(NO_3)_3 \bullet 9H_2O$-NaOH system using the controlled precipitation
784 method. Ingenieria e Investigación 30, 16-24.
785 Ryan, D.K., Weber, J.H., 1982. Fluorescence quenching titration for determination
786 of complexing capacities and stability constants of fulvic acid. Anal. Chem. 54,
787 986-990.
788 Sadrnourmohamadi, M., Gorczyca, B., 2015. Removal of dissolved organic carbon
789 (DOC) from hgh DOC and hardness water by chemical coagulation: relative
790 importance of monomeric, polymeric, and colloidal aluminum species.
791 Separation Sci. Technol. 50, 2075-2085.
792 https://doi.org/10.1080/01496395.2015.1014494.
793 Schaefer, J., Stejskal, E.O.R., 1976. Carbon-13 nuclear magnetic resonance of
794 polymers spinning at magic angle. J. Am. Chem. Soc. 98, 1031– 1032.
795 Schaller, J., Puppe, D., Kaczorek, D., Ellerbrock, R., Sommer, M., 2021. Silicon
796 cycling in soils revisited. Plants 10, 295.
797 https://doi.org/10.3390/plants10020295.
798 Scheinost, A.C., 2005. Metal oxides, in: Hillel D. (Ed.), Encyclopedia of soils in the
799 environment. Elsevier, Oxford, pp. 428-438. https://doi.org/10.1016/B0-12-
800 348530-4/00194-6.
801 Sharpless, C.M., McGown, L.B., 1999. Effects of aluminium-induced aggregation
802 on the fluorescence of humic substances. Env. Sci. Technol. 33, 3264–3270.
803 https://doi.org/10.1021/es981332v.
804 Shimizu, K., Morse, D.E., 2018. Silicatein: a unique silica-synthesizing catalytic triad
805 hydrolase from marine sponge skeletons and its multiple applications.
806 Methods Enzymol. 605, 429-455. https://doi.org/10.1016/bs.mie.2018.02.025
807 Shotyk, W., Sposito, G., 1988. Fluorescence quenching and aluminum
808 complexation by a chestnut leaf litter extract. Soil Sci. Soc. Am, J. 52, 1293–
809 1297. https://doi.org/10.2136/sssaj1988.03615995005200050014x.

Sommer, M., Kaczorek, D., Kuzyakov, Y., Breuer, J., 2006. Silicon pools and fluxes in soils and landscapes – a review. J. Plant Nutr. Soil Sci. 169, 310–329. https://doi.org/10.1002/jpln.200521981

Stevenson, F.J., Goh, K.M., 1971. Infrared spectra of humic acids and related substances. Geochim. Cosmochim. Acta 85, 471-485. https://doi.org/10.1016/0016-7037(71)90044-5.

Viers, J., Dupré, B., Polvé, M., Schott, J., Dandurand, J. L., Braun, J.J., 1997. Chemical weathering in the drainage basin of a tropical watershed (Nsimi-Zoetele site, Cameroon): comparison between organic poor and organic rich waters. Chem. Geol. 140, 181-206. https://doi.org/10.1016/S0009-2541(97)00048-X.

Viers, J., Dupré, B., Braun, J.-J., Deberdt, S., Angeletti, B., Ngoupayou, J.N., Michard, A., 2000. Major and trace element abundances, and strontium isotopes in the Nyong basin rivers (Cameroon): constraints on chemical weathering processes and elements transport mechanisms in humid tropical environments. Chem. Geol. 169, 211-241. https://doi.org/10.1016/S0009-2541(00)00298-9.

Wonisch, H., Gérard, F., Dietzel, M., Jaffrain, J., Nestroy, O., Boudot, J.-P., 2008. Occurrence of polymerized silicic acid and aluminum species in two forest soil solutions with different acidity. Geoderma 144, 435–445. https://doi.org/10.1016/j.geoderma.2007.11.022.

Yahya, Z., Abdullah, M.M.A.B., Hussin, K., Ismail, K.N., Razak, R.A., Sandu, A.V., 2015. Effect of solids-to-liquids, Na_2SiO_3-to-NaOH and curing temperature on the palm oil boiler ash (Si+Ca) geopolymerisation system. Materials 8, 2227-2242. https://doi.org/10.3390/ma8052227.

Yan, M., Benedetti, M.F., Korshin, G.V., 2013. Study of iron and aluminum binding to Suwannee River fulvic acid using absorbance and fluorescence spectroscopy: Comparison of data interpretation based on NICA-Donnan and Stockholm humic models. Water Res. 47, 5439-5446. https://doi.org/10.1016/j.watres.2013.06.022.

Zhao, K., Yang, Y., Peng, H., Zhang, L., Zhou, Y., Zhang, J., Du, C., Liu, J., Lin, X., Wang, N., Huang, H., Luo, L. (2022). Silicon fertilizers, humic acid and their impact on physicochemical properties, availability and distribution of heavy metals in soil and soil aggregates. Sci. Tot. Env. 153483. https://doi.org/10.1016/j.scitotenv.2022.153483.